

## Current fluctuations in boundary-driven quantum spin chains

Federico Carollo, Juan P. Garrahan, and Igor Lesanovsky

*School of Physics and Astronomy and Centre for the Mathematics and Theoretical Physics of Quantum Non-Equilibrium Systems,  
University of Nottingham, Nottingham, NG7 2RD, United Kingdom*

 (Received 20 February 2018; revised manuscript received 7 August 2018; published 5 September 2018)

Boundary-driven quantum spin chains are paradigmatic nonequilibrium systems featuring the presence of particle currents. In general, it may not be possible to distinguish an incoherent type of particle transport from a truly quantum coherent one through monitoring the mean current, as both ballistic as well as diffusive regimes occur in either setting. Here, we show that genuine coherent features become manifest in large fluctuations which allow a discrimination between incoherent and coherent quantum transport: in the former case, realizations that are characterized by atypically large boundary activity are associated with larger than typical currents, i.e., an enhanced number of events at the boundaries goes together with a large current. Conversely, in the coherent case the Zeno effect leads to the suppression of current in trajectories with large activity at the boundary. We analyze how these different dynamical regimes are reflected in the structure of rare fluctuations. We show moreover that realizations supporting a large current are generated via weak long-range correlations within the spin chain, typically associated with hyperuniformity. We further observe critical time-coexistence behaviors with intermittent currents in rare fluctuations of the strongly interacting XXZ chain for completely asymmetric drivings.

DOI: [10.1103/PhysRevB.98.094301](https://doi.org/10.1103/PhysRevB.98.094301)

### I. INTRODUCTION

Complex collective behavior of nonequilibrium systems admits a simplified thermodynamiclike description in terms of few macroscopic degrees of freedom [1–3]. These are usually time-averaged observables accounting for the response of the system to some quench or to some external driving [4–12]. For boundary-driven chains [cf. Figs. 1(a) and 1(b)], a complete characterization of the collective dynamics is achieved by considering the integrated current  $Q(t)$ , the net number of particles leaving the system through one of the boundaries up to time  $t$  and the activity  $K(t)$ , the total number of jumps at the same boundary. Typically, one is interested in average values of these quantities; however, interesting collective phenomena are often to be found in rare dynamical realizations [11, 13–17]. Moreover, the majority of studies on nonequilibrium systems focus on properties of the stationary state (see, e.g., [18–25]), and only a minority analyze rare dynamical behaviors [15, 26–29], mainly focused on the statistics of currents. In particular, much progress has been made in predicting the nonequilibrium behavior of different quantum and classical systems, unifying them in few classes according to the macroscopic emergent type of particle transport (e.g., diffusive, ballistic).

In specific cases, quantum systems with coherent transport have even been mapped to classical fully incoherent counterparts. For instance, it has been shown that the current statistics of the XX chain in the presence of dephasing coincides, in the thermodynamic limit, to the one of the classical symmetric exclusion process (SSEP) [27, 30]: the latter can be seen as a fully incoherent type of particle transport in the quantum spin chain, where the dynamics takes place among states that are diagonal in the number basis, with no quantum coherent features. The question that naturally arises from these results is thus whether there exist universal features in the rare events of quantum coherent nonequilibrium systems distinguishing

these from incoherent ones, or whether, at this macroscopic level, the microscopic nature of the dynamics becomes irrelevant.

In this work, we show that there is indeed one marked difference between coherent and incoherent transport in quantum boundary-driven chains and, irrespectively, of microscopic details of the dynamics and of the emergent collective behavior, a clear distinction between these two regimes can be established at the level of large fluctuations. We quantify the properties of dynamical fluctuations through the probability  $\pi_{K,Q}$  of a dynamical realization with activity  $K$  and current  $Q$ . For long times  $t$ , this probability obeys a so-called large deviation (LD) principle [1, 2], i.e.,  $\pi_{K,Q} \approx e^{-t\phi(k,q)}$ , where  $k(t) = t^{-1}K(t)$  and  $q(t) = t^{-1}Q(t)$ . The function  $\phi(k, q)$  is positive, and becomes zero when both its arguments  $k$  and  $q$  take the stationary state values  $\langle k \rangle$  and  $\langle q \rangle$ . Similarly, the conditional probability of a current  $Q$ , given an activity  $K$  is  $\pi_{Q|K} \approx e^{-t\phi|_k(q)}$ , with  $\phi|_k(q) = \phi(k, q) - \phi(k)$ , and  $\phi(k)$  being the LD function of the activity. In Figs. 1(c) and 1(d), we show this conditional LD function for paradigmatic incoherent (SSEP) and coherent (XX chain with dephasing) particle transport in the quantum chain, where the difference becomes obvious: for the incoherent case, an increasing activity leads to a larger than stationary *optimal current*, i.e., the most likely observed current for given activity. In the coherent case, instead, large activities lead to a smaller than stationary optimal current.

In the following, we consider in detail both quantum coherent boundary-driven spin chains (XX chain and XXZ chain) and their incoherent counterparts, which are represented by classical exclusion processes. For these models, we discuss the full range of fluctuations focusing, in particular, on the interplay between current and activity. Using perturbative arguments, we moreover establish that the features displayed in Fig. 1 are universal, i.e., they hold for any quantum spin chain

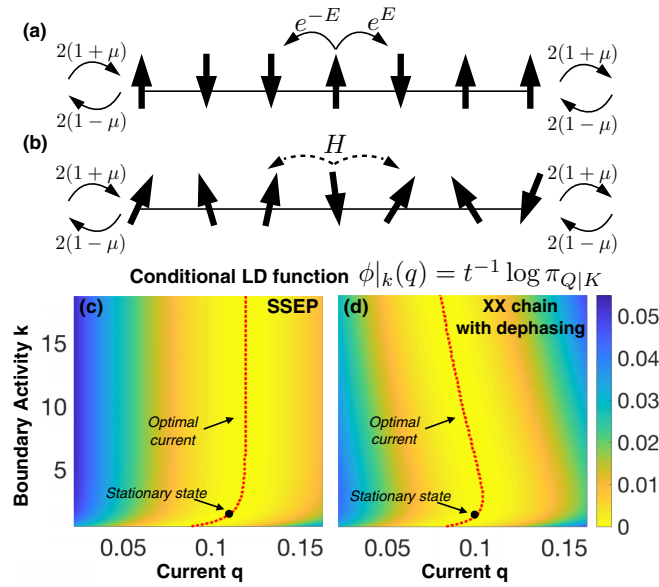


FIG. 1. (a) Incoherent chain: an up arrow indicates the presence of a particle. The latter jumps into neighboring sites only if these are empty, and rates can be asymmetric in the presence of a field  $E \neq 0$ . Particle injection/ejection takes place with boundary driving parameter  $\mu \in [0, 1]$ . This dynamics is equivalent to that of classical exclusion processes. (b) Coherent chain: transport is governed by a Hamiltonian  $H$ . Arrows with different angles pictorially indicate superposition states and the presence of quantum coherent effects. (c), (d) Exact numerical results for conditional large deviation (LD) function  $\phi|_k(q)$  of a system of  $L = 6$  sites,  $\mu = 0.6$ . The dashed line represents the most likely observed current  $q$  for different activities  $k$ ; bullets indicate the stationary state behavior. (c) SSEP with  $E = 0$ . (d) XX chain with dephasing showing suppression of the current for large activities.

Hamiltonian transport. Finally, we discuss how the distinct fluctuation behavior in the coherent and in the incoherent regime manifests in the spatial structure of particle trajectories.

## II. SPIN CHAIN MODELS AND DYNAMICAL LARGE DEVIATION FORMALISM

We briefly introduce the details of the formalism needed to derive the statistical properties of events mediated by the boundary driving. In order to obtain the joint current-activity statistics, it is convenient to work with the moment generating function  $\mathcal{Z}_{s,h} = \sum_{K,Q} e^{-sK+hQ} \pi_{K,Q}$ . This function not only provides all moments of the observables, but it can also be interpreted as the *dynamical partition function* of an ensemble of biased probabilities  $\pi_{K,Q}^{s,h} = e^{-sK+hQ} \pi_{K,Q}$ , favoring or disfavoring different realizations according to the value of the outcomes. These ensembles are associated to rare dynamical behaviors of the system, and are often used to describe properties of large fluctuations [14,31–33]. Indeed, for long times  $\mathcal{Z}_{s,h} \asymp e^{\psi(s,h)t}$ , and  $\psi(s,h)$  is the cumulant generating function (CGF) of the time-averaged quantities  $k(t)$ ,  $q(t)$  in both typical and biased ensembles of trajectories. As an example, while  $\langle q(t) \rangle = \partial_h \psi(s,h)|_{s,h=0}$  is the average current in the steady state,  $\langle q(t) \rangle_{s,h} = \partial_h \psi(s,h) = (t \mathcal{Z}_{s,h})^{-1} \sum_{K,Q} Q \pi_{K,Q}^{s,h}$  is the current in the  $s, h$  ensemble of rare trajectories. The

LD function  $\phi(k, q)$  can then be obtained via the Legendre transform  $\phi(k, q) = \max_{s,h} [-sk + hq - \psi(s, h)]$ .

We use this formalism here to study quantum spin- $\frac{1}{2}$  chains with  $L$  sites, and connected through their first and last sites to thermal reservoirs [see Figs. 1(a) and 1(b)]. For a coherent type of transport, we consider systems where the bulk dynamics is due to the Hamiltonian

$$H = \sum_{k=1}^{L-1} (\sigma_x^{(k)} \sigma_x^{(k+1)} + \sigma_y^{(k)} \sigma_y^{(k+1)} + \delta_z \sigma_z^{(k)} \sigma_z^{(k+1)}), \quad (1)$$

where  $\sigma_\alpha^{(k)}$  is the  $\alpha$  Pauli matrix of the  $k$ th spin. The external driving, describing dissipative particle injection/ejection at the boundary sites, is given by [34,35]

$$\begin{aligned} \mathcal{D}_{s,h}[\cdot] = & \sum_{\alpha=0}^1 \gamma_\alpha \left( L_\alpha^{(1)} \cdot L_\alpha^{(1)\dagger} - \frac{1}{2} \{ \cdot, (L_\alpha^\dagger L_\alpha)^{(1)} \} \right) \\ & + \sum_{\alpha=0}^1 \gamma_{1-\alpha} \left( e^{-s-(-1)^\alpha h} L_\alpha^{(L)} \cdot L_\alpha^{(L)\dagger} \right. \\ & \left. - \frac{1}{2} \{ \cdot, (L_\alpha^\dagger L_\alpha)^{(L)} \} \right), \end{aligned} \quad (2)$$

respectively,  $L_{0/1} = \sigma_\pm$ , and  $\gamma_{0/1} = 2(1 \pm \mu)$ , with  $\mu \in [0, 1]$  being the driving parameter. The fields  $s$  and  $h$ , conjugated respectively to the activity and to the current, are used, in the LD formalism, to obtain the CGF  $\psi(s, h)$  [15,26–28,36]. The latter is given by the eigenvalue with the largest real part of the so-called *tilted operator*  $\mathcal{L}_{s,h}[\cdot] = -i[H, \cdot] + \mathcal{D}_{s,h}[\cdot]$ .

We want to compare the fluctuations of the current due to the above Hamiltonian to those of a fully incoherent process. The latter, represented in Fig. 1(a), consists of classical particle jumps between different configurations which are diagonal in the basis of the number operators  $n^{(k)} = \sigma_+^{(k)} \sigma_-^{(k)}$ . Hence, this dynamics is clearly not characterized by any kind of quantum coherent feature. Considering that particles can only jump onto neighboring sites, such incoherent process is implemented by the following classical generator:

$$\begin{aligned} W_E = & \sum_{k=1}^{L-1} [e^E \sigma_+^{(k+1)} \sigma_-^{(k)} + e^{-E} \sigma_-^{(k+1)} \sigma_+^{(k)} \\ & - e^E n^{(k)} (\mathbf{1}_2 - n)^{(k+1)} - e^{-E} n^{(k+1)} (\mathbf{1}_2 - n)^{(k)}], \end{aligned} \quad (3)$$

where  $\mathbf{1}_2$  is the  $2 \times 2$  identity matrix, and the presence of an external field  $E \neq 0$  creates an asymmetry between the rates of bulk particle jumps to the left and to the right.

The effect of the boundary injection and ejection of particles are accounted for by the term

$$\begin{aligned} W_{s,h}^{\text{bound}} = & \gamma_0 [\sigma_+ - (\mathbf{1}_2 - n)]^{(1)} + \gamma_1 [\sigma_- - n]^{(1)} \\ & + \gamma_1 [e^{-s-h} \sigma_+ - (\mathbf{1}_2 - n)]^{(L)} \\ & + \gamma_0 [e^{-s+h} \sigma_- - n]^{(L)}. \end{aligned} \quad (4)$$

For this incoherent process, the generator  $W^{\text{tot}} = W_E + W_{0,0}^{\text{bound}}$  implements the dynamics of the probability vector of the particle configurations. The modified operator  $W_{s,h}^{\text{tot}} = W_E + W_{s,h}^{\text{bound}}$ , on the other hand, constitutes the tilted operator from which all cumulants of the chosen observables are extracted.

It is important to notice that the incoherent processes presented here are nothing but classical simple exclusion processes: in particular, for  $E = 0$  the dynamics is that of the SSEP, while for  $E \neq 0$  one has the asymmetric simple exclusion process (ASEP). Notice also that, as discussed in [36–38], these processes could be equivalently represented in a fully quantum framework by means of a specific, uniquely dissipative, bulk dynamics. This highlights how the classical simple exclusion dynamics represents the incoherent counterpart of the bulk dynamics governed by quantum Hamiltonians.

### III. CURRENT FLUCTUATIONS IN THE XX CHAIN

We start by considering the XX chain, where the coherent bulk dynamics is governed by the Hamiltonian given by Eq. (1) with  $\delta_z = 0$ . This is a noninteracting ballistic system. In order to compute  $\psi(s, h)$ , we exploit that the map  $\mathcal{L}_{s,h}[\cdot]$  can be cast into the non-Hermitian operator [26,39,40]

$$\hat{\mathcal{L}}_{s,h} = \mathbf{a} \cdot U^\dagger \begin{pmatrix} X & 0 \\ 0 & -X^T \end{pmatrix} U \cdot \mathbf{a} - 4, \quad U = \frac{1}{\sqrt{2}} \begin{pmatrix} 1 & -i \\ 1 & i \end{pmatrix}. \quad (5)$$

Here,  $\mathbf{a}$  is a  $4L$ -dimensional vector, whose entries  $\mathbf{a}_i$  are fermionic Majorana operators,  $\{\mathbf{a}_i, \mathbf{a}_j\} = \delta_{i,j}$ , and the matrix  $X$  contains the details of the tilted dynamics (see Appendix A for details). The operator can then be brought into a diagonal form  $\hat{\mathcal{L}}_{s,h} = 2 \sum_{m=1}^{2L} \Lambda_m b'_m b_m - 4$ , in terms of normal modes  $b_m, b'_m$ , where  $\Lambda_m$  are the eigenvalues of the matrix  $X$  [39,40]. The CGF is therefore  $\psi(s, h) = 2 \sum_{m \in \Lambda^+} \text{Re}(\Lambda_m) - 4$ , with  $\Lambda^+$  being the set of  $m$  for which  $\text{Re}(\Lambda_m) > 0$ . Associated to this, one has the left and right eigenvectors  $\langle \mathbf{L}_{s,h} | = \langle \hat{0} | \prod_{m \in \Lambda^+} b_m, | \mathbf{R}_{s,h} \rangle = \prod_{m \in \Lambda^+} b'_m | 0 \rangle$ , with  $\langle \hat{0} |, | 0 \rangle$  being the left, respectively, right vacuum.

Using this formalism one can show that, in the large- $L$  limit, the magnitude of the current is always bounded by the value  $4/\pi$ . This was noticed in [26] for the current statistics, but we see here that this bound is present for any activity, even when the latter is atypically large. Moreover, Fig. 2(a) shows the same suppression of the optimal current for increasing activities that we already discussed in presence of dephasing [Fig. 1(d)]. This

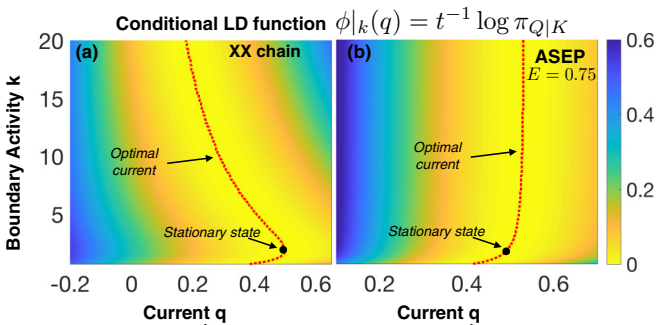


FIG. 2. Exact numerical results for the conditional LD function  $\phi|_k(q)$ : the dashed lines indicate the most likely value of the current, points instead the stationary state behavior. (a) XX chain  $L = 100$  for  $\mu = 0.5$ . (b) Classical ballistic asymmetric exclusion process (ASEP), for  $L = 6$ ,  $\mu = 0.5$ , and  $E = 0.75$ .

appears to be a signature of the coherent nature of the quantum transport in these large fluctuations, independent on whether currents are ballistic or diffusive.

### IV. CURRENT FLUCTUATIONS AND THE ZENO EFFECT

We will now investigate to what extent the previous findings generalize, and, in particular, whether they apply also to interacting systems. To address this situation, it is convenient to move from the description of events with fixed  $k$  and  $q$ , given by the LD function  $\phi(k, q)$ , to the one based on biased ensembles of probabilities, where average values are under control [14,32,33,41]. This means that we focus on the CGF  $\psi(s, h)$ . With this description, we can compute the current  $\langle q(t) \rangle_{s,h}$  in biased ensembles and recover our previous findings observing its behavior for different values of the biases: the XX chain displays an eventual current suppression in ensembles with increasing activities ( $s < 0$ ) [see Fig. 3(a)], while for the SSEP, representing the incoherent transport in the quantum chain, a larger average number of events at the boundary favors an increased net flow of particles [see Fig. 3(b)].

Let us now consider the quantum XXZ chain for  $\mu \neq 1$ , whose Hamiltonian is the one of Eq. (1) with finite value of  $\delta_z$ . This system undergoes a phase transition controlled by the anisotropy  $\delta_z$  [12,28], from ballistic ( $\delta_z < 1$ ) to diffusive ( $\delta_z > 1$ ) transport, and further presents anomalous current fluctuations in the diffusive regime [28]. It is the simplest, yet nontrivial, model that we can exploit to understand whether the presence of interactions in the Hamiltonian changes the rare behavior of quantum spin chains. For  $\mu = 0$ , we observe, in the ballistic phase, that active and inactive ensembles, characterized by the same  $|s|$ , show the same suppressed value of the current as it happens for the XX chain. In the diffusive regime [Fig. 3(c)], for small biases towards active realizations, currents tend to increase with the activity, as it happens for incoherent processes. However, in very active ensembles, there is a departure from the incoherent diffusive behavior, manifested in the suppression of the current. Since we observe the same for the XX chain with dephasing at the same  $\mu = 0$ , this particular behavior with  $s$  seems to be related to the diffusive regime more than to the presence of interactions in the Hamiltonian. We further considered the ASEP with finite field  $E$ . This model is ballistic [42–44], but, contrary to the coherent ballistic case, larger activities are associated to larger currents [cf. Fig. 2(b)].

All these findings lead us to the following conclusion: in boundary-driven spin chains quantumness manifests in a particular behavior of dynamical fluctuations, which is not dependent on whether the average transport is ballistic or diffusive. The origin of this is the Zeno effect: this not only affects stationary properties (see also, e.g., [45,46]), but also very active dynamical realizations, where sites at the boundaries of the chain are repeatedly disturbed by particle injection or ejection from the reservoir and, as a consequence, the quantum coherent transport is frozen. Via perturbation theory on the tilted operator, we can extend our numerical findings to quantum spin chains with generic Hamiltonians. Indeed, we find that, with or without bulk dephasing,  $\forall \mu \neq 1$  and  $\forall L$ , particle transport is suppressed for ensembles with

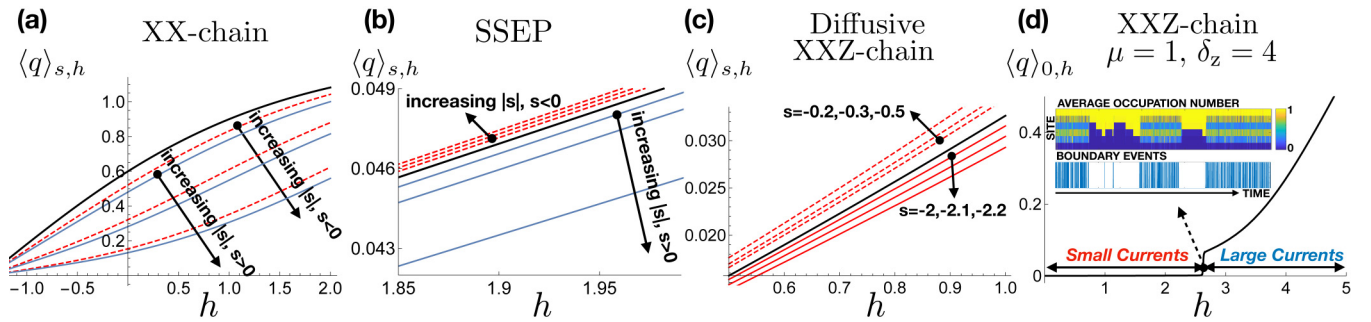


FIG. 3. Exact numerical results for the current  $\langle q(t) \rangle_{s,h}$  computed with probabilities  $\pi_{k,Q}^{s,h}$ , biasing dynamical realizations according to the value of current and activity. Thick black lines are for typical (nonbiased) activity. (a) XX chain  $\mu = 0.6$ ,  $|s| = 1, 2, 3$ : dashed lines are for active ensembles, solid lines for inactive ones. (b) SSEP  $L = 21$ ,  $|s| = 0.5, 1, 2$ ,  $\mu = 0$ : dashed lines are for active ensembles, solid lines for inactive ones. (c) XXZ chain  $\delta_z = 4$ ,  $L = 8$ ,  $\mu = 0$ . Active ensembles: for small  $|s|$  currents increase while for large  $|s|$  are suppressed. (d) XXZ chain  $\delta_z = 4$ ,  $L = 6$ ,  $\mu = 1$ . Crossover from small to large current regime. A dynamical trajectory at the critical point shows that fluctuations, breaking the clustered insulating structure of the density profile, are sustained for finite time windows and determine intermittency of the current.

very large average activity ( $s \rightarrow -\infty$ ) (see Appendix B):

$$\lim_{s \rightarrow -\infty} \langle q(t) \rangle_{s,h} = 0.$$

As this result is independent of the specific system's Hamiltonian, we have shown that this current suppression is a universal feature of spin chains with a truly quantum coherent particle transport in the bulk. Moreover, for  $|s| \gg h$ , the time-averaged activity  $\langle k(t) \rangle_{s,h} \propto e^{-s}$ , and one has  $\langle q(t) \rangle_{s,h} \propto \frac{1}{\langle k(t) \rangle_{s,h}}$ , showing a diffusivelike scaling of the particle transport with the average rate of events at the boundary.

We conclude this section by highlighting a critical behavior in the current fluctuations of the XXZ chain. The current suppression for coherent quantum transport that we have discussed so far takes only place when  $\mu \neq 1$ . Indeed, if  $\mu = 1$  the rightmost boundary can only extract particles [Fig. 1(b)] and thus fluctuations with larger activity are clearly sustaining larger than stationary currents: for this value of  $\mu$ , current and activity are the same observable. While, in general, current fluctuations in this case do not show particular behaviors (see, e.g., [26]), in this case, we found that the strongly interacting XXZ chain displays a critical behavior reminiscent of first-order phase transitions: current fluctuations undergo a steep crossover from typical low current [25] to atypical large current regime [Fig. 3(d)]. At the critical point we observe intermittent currents: the cluster structure of the density profile, responsible for very small currents [25], alternates in time with fluctuations breaking the clusters and allowing for particle transport.

## V. COMPETITION BETWEEN CURRENT SUPPRESSION IN ACTIVE FLUCTUATIONS AND EMERGENT INCOHERENT TRANSPORT

Many quantum coherent models display emergent incoherent dynamics in some limiting case. A common scenario is when the coherent bulk dynamics is affected by the presence of an environment which introduces strong dephasing. It is thus of interest to investigate how the competition between current suppression, intrinsic in the coherent nature of boundary-driven transport models, and the current enhancement of incoherent processes manifests in dynamical fluctuations.

In this section we explore this by considering a well-known example: the boundary-driven XX chain in the presence of dephasing. The dynamics of this system is generated by the following master equation:

$$\partial_t \rho_t = -i[H, \rho_t] + \mathcal{D}_{0,0}[\rho_t] + \mathcal{L}^D[\rho_t],$$

where the Hamiltonian  $H$  is as in Eq. (1) with  $\delta_z = 0$  and  $\mathcal{L}^D$  describes the presence of a dephasing environment in the bulk, which is accounted for by the term

$$\mathcal{L}^D[\rho] = \gamma_D \sum_{m=1}^L \left( n^{(m)} \rho n^{(m)} - \frac{1}{2} \{ \rho, n^{(m)} \} \right).$$

For  $\gamma_D = 0$  this quantum model can be considered as purely coherent, while in the presence of strong dephasing rates  $\gamma_D \gg 1$  it is known that its dynamics is effectively equivalent to that of the incoherent SSEP (see, e.g., [47]). Therefore, by varying the strength of dephasing, it is possible to interpolate between a *fully quantum* coherent behavior ( $\gamma_D = 0$ ) and an emergent incoherent one ( $\gamma_D \gg 1$ ).

In Fig. 4, we compare the conditional large deviation functions  $\phi_k(q)$  obtained for different values of the dephasing rate  $\gamma_D$ . This figure clearly displays how for increasing dephasing rates the suppression of the optimal current is moved towards larger and larger values of the boundary activity. This fact is witnessing the competition between the quantum Zeno effect affecting the coherent particle transport and the emergent incoherent behavior of the model. The latter delays the appearance of the current suppression and makes current fluctuations of this system behave like those of an incoherent process in larger and larger parameter regions above the stationary activity value.

## VI. SPATIAL STRUCTURE OF TRAJECTORIES

Now that we know how large fluctuations allow to discriminate between coherent and incoherent particle transport in boundary-driven quantum spin chains, it is interesting to understand their spatial configuration. A key quantity capturing relevant features of density correlations is the structure factor

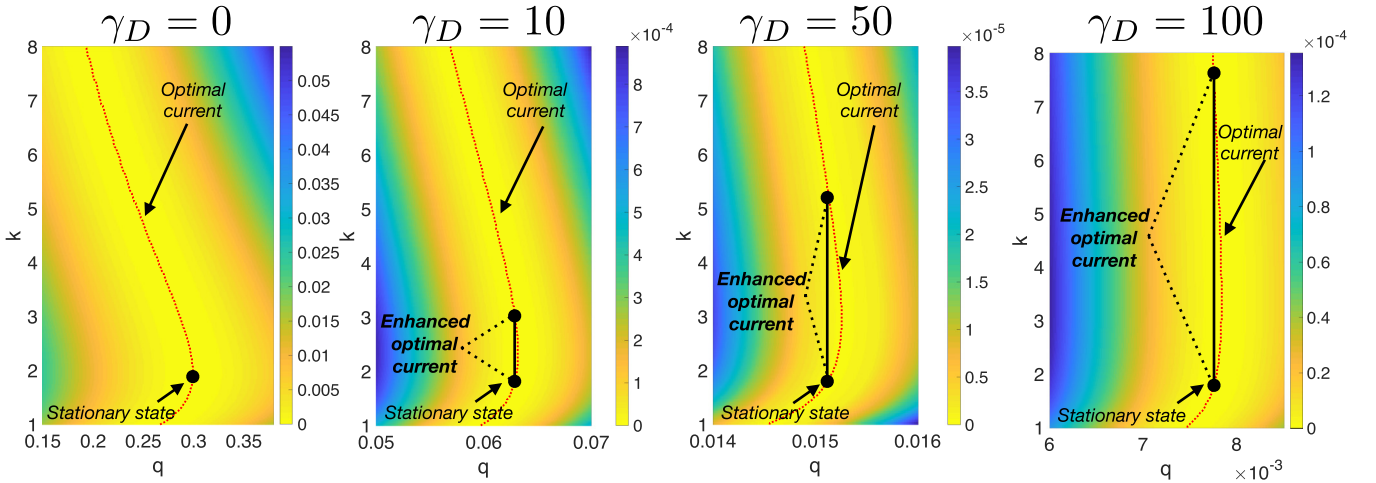


FIG. 4. Plot of the conditional large deviation function  $\phi_k(q)$  for an XX chain of  $L = 4$  qubits in the presence of bulk dephasing with rate  $\gamma_D$ , and driving parameter  $\mu = 0.3$ . When  $\gamma_D = 0$  (fully coherent case), for this value of  $\mu$  we see that the stationary state current is also the largest possible optimal current, so that fluctuations with larger than typical boundary activity can only lead to current suppression. For larger and larger  $\gamma_D$ , instead, it is possible to identify an increasing region of active fluctuations where the optimal current is enhanced with respect to the stationary one. Eventually, for very large boundary activities the Zeno effect manifests and leads to current suppression. The fact that the optimal current suppression starts to appear for larger and larger boundary activities when increasing the dephasing rate  $\gamma_D$  is thus a manifestation of the emergent classical incoherent behavior of the quantum XX chain with strong dephasing competing with the quantum Zeno effect.

[10,17,30,48]

$$S(p) := \frac{2}{L} \sum_{m,k=1}^L \sin(k p) \sin(m p) C_{mk}(s, h),$$

with  $p = \frac{\pi}{L} p'$ , for  $p' = 1, 2, \dots, L-1$ , and  $C_{mk}(s, h)$  the density-density covariance matrix in the biased  $s, h$  ensemble of trajectories. Defining the expectation  $\langle O \rangle_{s,h} = \text{Tr}(O \ell_{s,h}^{1/2} r_{s,h} \ell_{s,h}^{1/2})$ , with  $\ell_{s,h}, r_{s,h}$  the left, respectively right, eigenmatrix of the tilted operator  $\mathcal{L}_{s,h}$  associated to the eigenvalue  $\psi(s, h)$ , the density-density correlations can be computed as [15,30,36]

$$C_{mk}(s, h) = \langle n_m n_k \rangle_{s,h} - \langle n_m \rangle_{s,h} \langle n_k \rangle_{s,h}.$$

For the XX chain, reconstructing the matrices  $r_{s,h}, \ell_{s,h}$  from the fermionic formulation is not an easy task. Nonetheless, we can very well approximate these correlations with  $C_{mk}(s, h) \approx \langle \langle n_m n_k \rangle \rangle_{s,h} - \langle \langle n_m \rangle \rangle_{s,h} \langle \langle n_k \rangle \rangle_{s,h}$  (see Appendix C), where  $\langle \langle O \rangle \rangle_{s,h} = \text{Tr}(\ell_{s,h} O r_{s,h})$ . This functional can be computed in the fermionic language as  $\langle \langle O \rangle \rangle_{s,h} = \langle \mathbf{L}_{s,h} | O(\mathbf{a}) | \mathbf{R}_{s,h} \rangle$ , with  $O(\mathbf{a})$  being the operator  $O$  written in terms of Majorana fermions.

Density correlations in the typical steady-state dynamics of the XX chain are extended at most to nearest neighbors [18]. Very different is the behavior for increasing values of the current bias  $h$ : in these ensembles, characterized by large currents, we observe very weak but longer range correlations spread all along the chain. These have the usual anticorrelated structure suppressing density fluctuations and signaling hyperuniformity [10,49] (see Fig. 5). Conversely, when favoring trajectories with a large number of boundary events, density correlations are destroyed. In very active ensembles ( $|s| \gg |h|$ ), the system tends to be completely uncorrelated, with an almost flat structure factor. The same happens also for  $\delta_z > 0$

and in the presence of dephasing: large activities break the long-range correlations necessary to sustain efficient particle transport. In stark contrast, in very active realizations of boundary-driven quantum spin chains with incoherent bulk transport density correlations are not diminished.

The strongly interacting XXZ chain shows also here an anomalous behavior. In dynamical fluctuations with large currents, one witnesses the buildup of anticorrelations between nearest neighbors. However, the presence of strong interactions leaves all other sites positively correlated, as it happens in the stationary state [50], and, as a consequence, the structure factor is not signaling hyperuniformity.

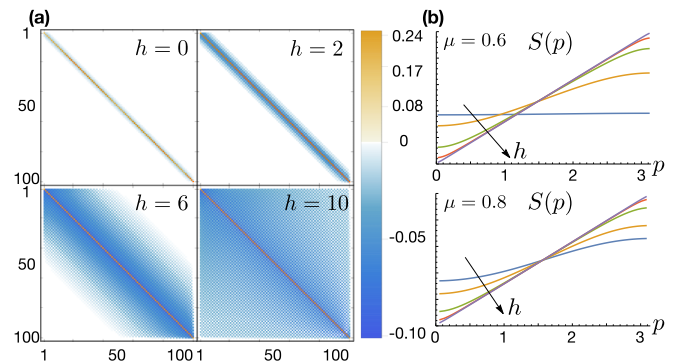


FIG. 5. (a) Density correlations  $C_{mk}$  for  $\mu = 0.6$ , bias  $s = -3$ ,  $L = 100$ , and different values of  $h$ . Favoring realizations with large currents we observe how long-range (anti)correlations are developed. (b) Structure factor  $S(p)$  with a linear behavior, for small  $p$  in large current events, signaling hyperuniformity. Top:  $s = -3$ ,  $\mu = 0.6$ , and  $h = 0, 3, 5, 7, 10$ ,  $L = 100$ . Bottom:  $s = 0$ ,  $\mu = 0.8$ , and  $h = 0, 1, 3, 5, 7$ ,  $L = 50$ .

## VII. CONCLUSIONS

We conducted a systematic exploration of large fluctuations in quantum spin chains characterized by both a coherent and an incoherent type of particle transport in the bulk. Our results show that the coherent/incoherent nature of the particle transport is not apparent from the typical behavior of the dynamics but only becomes apparent after a careful examination of dynamical fluctuations. We have further highlighted a critical behavior appearing in the current fluctuations of the strongly interacting XXZ chain for fully asymmetric driving. For this system, current fluctuations feature a first-order transitionlike behavior, with critical dynamical realizations that are a mixture of two very different dynamical phases.

## ACKNOWLEDGMENTS

The research leading to these results has received funding from the European Research Council under the European Unions Seventh Framework Programme (FP/2007-2013)/ERC Grant Agreement No. 335266 (ESCQUMA), and the EPSRC Grant No. EP/M014266/1. I.L. gratefully acknowledges funding through the Royal Society Wolfson Research Merit Award.

## APPENDIX A: CUMULANT GENERATING FUNCTION OF THE XX CHAIN

In this appendix, we will briefly show how to write the tilted operator for the XX chain in the third quantization formalism [26,39,40] and compute its eigenvalue with largest real part. Introducing, via Jordan-Wigner transformation, the Majorana operators for  $k = 1, 2, \dots, L$ ,

$$w_{2k-1} = \sigma_x^{(k)} \prod_{h=1}^{k-1} \sigma_z^{(h)}, \quad w_{2k} = \sigma_y^{(k)} \prod_{h=1}^{k-1} \sigma_z^{(h)}, \quad (\text{A1})$$

such that  $\{w_k, w_h\} = 2\delta_{k,h}$ , one can write the XX-chain Hamiltonian as

$$H = -i \sum_{k=1}^{L-1} (w_{2k} w_{2k+1} - w_{2k-1} w_{2k+2}).$$

Also, jump operators appearing in the boundary dissipative contribution can be written in the following way:

$$\begin{aligned} \sigma_+^{(1)} &= \frac{1}{2}(w_1 + iw_2), & \sigma_-^{(1)} &= \frac{1}{2}(w_1 - iw_2), \\ \sigma_+^{(L)} &= -Z(w_{2L-1} + iw_{2L}), & \sigma_-^{(L)} &= -Z(w_{2L-1} - iw_{2L}), \end{aligned} \quad (\text{A2})$$

where  $Z$ , the parity operator, is  $Z = \prod_{k=1}^L \sigma_z^{(k)}$ .

With the help of the Majorana fermions, we can as well construct a basis for the space of operators. A generic element of such a basis reads as

$$B_{\vec{\alpha}} = \prod_{k=1}^{2L} w_k^{\alpha_k}, \quad \text{with } \alpha_k = 0, 1.$$

Through these elements, one can define a vector space formed by the vectors  $|B_{\vec{\alpha}}\rangle$ , and embedded with the inner product  $\langle B_{\vec{\beta}} | B_{\vec{\alpha}} \rangle = \frac{1}{2^L} \text{Tr}(B_{\vec{\beta}}^\dagger B_{\vec{\alpha}})$ . Focusing on the even subspace of

these operators  $B_{\vec{\alpha}}$  (namely, the ones for which  $\sum_k \alpha_k$  is an even number), which is preserved by the action of the tilted operator  $\mathcal{L}_{s,h}$ , and on which the action of  $Z$  is trivial, one can show [26,39,40] that  $\mathcal{L}_{s,h}$  can be written as a linear map

$$\hat{\mathcal{L}}_{s,h} = \hat{\mathbf{a}} \cdot A \cdot \hat{\mathbf{a}} - 4,$$

acting on the corresponding (even) vector subspace.  $A$  is the so-called shape matrix, and the vector  $\hat{\mathbf{a}}$  is a vector of  $4L$  new Majorana operators  $\{\hat{\mathbf{a}}_h, \hat{\mathbf{a}}_k\} = \delta_{h,k}$ , such that

$$\sqrt{2} \hat{\mathbf{a}}_{2k-1} |B_{\vec{\alpha}}\rangle = |w_k B_{\vec{\alpha}}\rangle, \quad k = 1, 2, \dots, 2L.$$

The shape matrix  $A$ , for the considered tilted operator, assumes the following form (coinciding for  $s = 0$  to what is found in [26]):

$$A = \begin{pmatrix} \hat{B}_{0,0}(-\mu) & \hat{H} & \mathbf{0} & \dots & \dots & \mathbf{0} \\ \hat{H} & \mathbf{0} & \hat{H} & \ddots & \ddots & \mathbf{0} \\ \mathbf{0} & \hat{H} & \mathbf{0} & \ddots & \ddots & \mathbf{0} \\ \vdots & \ddots & \ddots & \ddots & \ddots & \vdots \\ \vdots & \ddots & \ddots & \ddots & \mathbf{0} & \hat{H} \\ \mathbf{0} & \mathbf{0} & \mathbf{0} & \dots & \hat{H} & \hat{B}_{s,h}(\mu) \end{pmatrix},$$

with  $\hat{H} = i\sigma_y \otimes \mathbf{1}_2$ , and

$$\begin{aligned} \hat{B}_{s,h}(\mu) &= f_{s,h}^1(\mu) \sigma_y \otimes \sigma_z + f_{s,h}^2(\mu) \sigma_y \otimes \sigma_x \\ &\quad + f_{s,h}^3(\mu) \mathbf{1}_2 \otimes \sigma_y, \end{aligned}$$

together with

$$\begin{aligned} f_{s,h}^1(\mu) &= -\mu, \\ f_{s,h}^2(\mu) &= -ie^{-s}[\mu \cosh(h) + \sinh(h)], \\ f_{s,h}^3(\mu) &= -e^{-s}[\cosh(h) + \mu \sinh(h)]. \end{aligned} \quad (\text{A3})$$

This matrix can be written in a tensor product form

$$\begin{aligned} A &= f_{0,0}^1(-\mu) D_1 \otimes \sigma_y \otimes \sigma_z + f_{0,0}^2(-\mu) D_1 \otimes \sigma_y \otimes \sigma_x \\ &\quad + f_{0,0}^3(-\mu) D_1 \otimes \mathbf{1}_2 \otimes \sigma_y + \tilde{H} \otimes \hat{H} \\ &\quad + f_{s,h}^1(\mu) D_L \otimes \sigma_y \otimes \sigma_z + f_{s,h}^2(\mu) D_L \otimes \sigma_y \otimes \sigma_x \\ &\quad + f_{s,h}^3(\mu) D_L \otimes \mathbf{1}_2 \otimes \sigma_y, \end{aligned}$$

where  $(D_N)_{m,k} = \delta_{k,N} \delta_{k,m}$  and with  $\tilde{H}$  being the  $L \times L$  matrix whose nonzero elements are only  $\tilde{H}_{k,k+1} = \tilde{H}_{k-1,k} = 1$ . All terms have, as second entry of the tensor product, either an identity or a  $\sigma_y$ . It proves therefore convenient to reshape the above matrix moving the second and the third entries of the tensor product to the first, respectively, second position. In this new representation the matrix reads as

$$\begin{aligned} A' &= f_{0,0}^1(-\mu) \sigma_y \otimes \sigma_z \otimes D_1 + f_{0,0}^2(-\mu) \sigma_y \otimes \sigma_x \otimes D_1 \\ &\quad + f_{0,0}^3(-\mu) \mathbf{1}_2 \otimes \sigma_y \otimes D_1 + i\sigma_y \otimes \mathbf{1}_2 \otimes \tilde{H} \\ &\quad + f_{s,h}^1(\mu) \sigma_y \otimes \sigma_z \otimes D_L + f_{s,h}^2(\mu) \sigma_y \otimes \sigma_x \otimes D_L \\ &\quad + f_{s,h}^3(\mu) \mathbf{1}_2 \otimes \sigma_y \otimes D_L. \end{aligned}$$

Now, we apply a rotation on the first term of the tensor product, bringing  $\sigma_y$  to its diagonal form ( $U\sigma_y U^\dagger = \sigma_z$ , with  $U$  as in

the main text), obtaining

$$\begin{aligned} A'' &= \mathbf{1}_2 \otimes \sigma_y \otimes (f_{0,0}^3(-\mu)D_1 + f_{s,h}^3(\mu)D_L) \\ &+ \sigma_z \otimes (f_{0,0}^1(-\mu)\sigma_z \otimes D_1 + f_{0,0}^2(-\mu)\sigma_x \otimes D_1) \\ &+ i\mathbf{1}_2 \otimes \tilde{H} + f_{s,h}^1(\mu)\sigma_z \otimes D_L + f_{s,h}^2(\mu)\sigma_x \otimes D_L. \end{aligned}$$

We can then collect terms introducing a matrix  $X$ , so that one has

$$A'' = \begin{pmatrix} X & 0 \\ 0 & -X^T \end{pmatrix};$$

the matrix  $X$  is given by  $X = \mathbf{1}_2 \otimes i\tilde{H} + \Gamma_1 + \Gamma_L$ , with  $\Gamma_1 = B_{0,0}(-\mu) \otimes D_1$  and  $\Gamma_L = B_{s,h}(\mu) \otimes D_L$ , where

$$B_{s,h}(\mu) = \begin{pmatrix} -\mu & -ie^{-(s+h)}(\mu-1) \\ -ie^{-(s-h)}(\mu+1) & \mu \end{pmatrix}.$$

The reordering that we performed on the tensor product affects also the vector of Majorana fermions  $\hat{\mathbf{a}}$ . This can be accounted for by introducing a new vector  $\mathbf{a}$ , made as follows:

$$\begin{aligned} \mathbf{a} &= (\hat{\mathbf{a}}_1, \hat{\mathbf{a}}_5, \hat{\mathbf{a}}_9, \dots, \hat{\mathbf{a}}_{1+4(L-1)}, \hat{\mathbf{a}}_2, \hat{\mathbf{a}}_6, \hat{\mathbf{a}}_{10}, \dots, \hat{\mathbf{a}}_{2+4(L-1)}, \\ &\times \hat{\mathbf{a}}_3, \hat{\mathbf{a}}_7, \hat{\mathbf{a}}_{11}, \dots, \hat{\mathbf{a}}_{3+4(L-1)}, \hat{\mathbf{a}}_4, \hat{\mathbf{a}}_8, \hat{\mathbf{a}}_{12}, \dots, \hat{\mathbf{a}}_{4L})^T. \end{aligned}$$

This shows that the generator can be written as in Eq. (5) of the main text:

$$\hat{\mathcal{L}}_{s,h} = \mathbf{a} \cdot U^\dagger \begin{pmatrix} X & 0 \\ 0 & -X^T \end{pmatrix} U \cdot \mathbf{a} - 4.$$

We now want to find the largest real eigenvalue of the above generator. Assuming  $X$  to be diagonalizable, there exists a matrix  $P$ , such that  $X = P\Lambda P^{-1}$ , with  $\Lambda$  diagonal; thus,

$$\begin{aligned} U^\dagger \begin{pmatrix} X & 0 \\ 0 & -X^T \end{pmatrix} U &= U^\dagger \begin{pmatrix} P & 0 \\ 0 & P^{-T} \end{pmatrix} \\ &\times \begin{pmatrix} \Lambda & 0 \\ 0 & -\Lambda \end{pmatrix} \begin{pmatrix} P^{-1} & 0 \\ 0 & P^T \end{pmatrix} U. \end{aligned}$$

Defining  $V = \begin{pmatrix} P^{-1} & 0 \\ 0 & P^T \end{pmatrix} U$ , with analogous calculation to those of Ref. [40], one finds

$$\hat{\mathcal{L}}_{s,h} = \mathbf{a} \cdot V^T \begin{pmatrix} 0 & -\Lambda \\ \Lambda & 0 \end{pmatrix} V \cdot \mathbf{a} - 4.$$

The matrix  $V$  implements a generalized rotation acting on the vector  $\mathbf{a}$ , in such a way that it introduces  $4L$  almost canonical fermionic creation and annihilation operators

$$\begin{pmatrix} b \\ b' \end{pmatrix} = V \cdot \mathbf{a},$$

obeying  $\{b_h, b'_k\} = \delta_{h,k}$ , and with all other anticommutation relations being zero. These creation and annihilation operators are the normal master modes of the tilted operator. With these, one finds

$$\hat{\mathcal{L}}_{s,h} = \sum_{j=1}^{2L} \Lambda_j (b'_j b_j - b_j b'_j) - 4,$$

and using the anticommutation relations

$$\hat{\mathcal{L}}_{s,h} = 2 \sum_{j=1}^{2L} \Lambda_j b'_j b_j - 4 - \sum_{j=1}^{2L} \Lambda_j = 2 \sum_{j=1}^{2L} \Lambda_j b'_j b_j - 4,$$

where the last equality comes from the fact that  $X$  is traceless. The dependence on the biases  $s, h$  and on the parameter  $\mu$  is encoded in the eigenvalues  $\Lambda_j$  of the matrix  $X$ , as well as in the rotation matrix  $V$ . Introducing right and left vacuum  $|0\rangle, \langle\bar{0}|$ , which are annihilated by  $b_m$  and  $b'_m$ , respectively, one finds that the eigenvalue with the largest real part corresponds to the right eigenvector  $|\mathbf{R}_{s,h}\rangle = \prod_{m \in \Lambda^+} b'_m |0\rangle$ , as well as to the left one  $\langle\mathbf{L}_{s,h}| = \langle\bar{0}| \prod_{m \in \Lambda^+} b_m$ , and is given by

$$\psi(s, h) = 2 \sum_{m \in \Lambda^+} \text{Re}(\Lambda_m) - 4,$$

with  $\Lambda^+$  being the set of  $m$  for which  $\text{Re}(\Lambda_m) > 0$ .

## APPENDIX B: PERTURBATION THEORY ON THE TILTED OPERATOR

Let us start by writing explicitly all terms of the tilted operator  $\mathcal{L}_{s,h}$  with a generic Hamiltonian  $H$ :

$$\begin{aligned} \mathcal{L}_{s,h}[\rho] &= -i[H, \rho] + \gamma_0 \sigma_+^{(1)} \rho \sigma_-^{(1)} - \frac{\gamma_0}{2} \{\rho, \sigma_-^{(1)} \sigma_+^{(1)}\} \\ &+ \gamma_1 \sigma_-^{(1)} \rho \sigma_+^{(1)} - \frac{\gamma_1}{2} \{\rho, \sigma_+^{(1)} \sigma_-^{(1)}\} \\ &+ e^{-s} [\gamma_1 e^{-h} \sigma_+^{(L)} \rho \sigma_-^{(L)} + \gamma_0 e^h \sigma_-^{(L)} \rho \sigma_+^{(L)}] \\ &- \frac{\gamma_1}{2} \{\rho, \sigma_-^{(L)} \sigma_+^{(L)}\} - \frac{\gamma_0}{2} \{\rho, \sigma_+^{(L)} \sigma_-^{(L)}\}. \quad (\text{B1}) \end{aligned}$$

For large negative  $s$  we see that there is a part of the above map which is predominant. Defining

$$\mathcal{K}[\rho] = [\gamma_1 e^{-h} \sigma_+^{(L)} \rho \sigma_-^{(L)} + \gamma_0 e^h \sigma_-^{(L)} \rho \sigma_+^{(L)}],$$

and collecting in  $\mathcal{W}[\rho]$  all remaining terms appearing on the right-hand side of Eq. (B1), we can write the tilted operator as

$$\mathcal{L}_{s,h}[\rho] = e^{-s} \mathcal{K}[\rho] + \mathcal{W}[\rho].$$

When considering large negative  $s$ ,  $\mathcal{L}_{s,h} = e^{|s|} (\mathcal{K} + e^{-|s|} \mathcal{W})$ , with  $e^{-|s|}$  a small number, showing that we can apply perturbation theory in order to consider the correction to the dominant term  $\mathcal{K}$  due to the map  $\mathcal{W}$ . To proceed, one needs first to diagonalize the map  $\mathcal{K}$ . This acts in a nontrivial way only on the last site of the chain; we therefore consider operators of the form  $x \otimes y$ , where  $x$  is an operator acting on the first  $L-1$  sites of the chain, while  $y$  acts only on the last one. We thus have

$$\begin{aligned} \mathcal{K}[x \otimes y] &= x \otimes \hat{\mathcal{K}}[y], \\ \hat{\mathcal{K}}[y] &= [\gamma_1 e^{-h} \sigma_+ y \sigma_- + \gamma_0 e^h \sigma_- y \sigma_+]. \end{aligned}$$

It can be shown that the largest eigenvalue of the map  $\hat{\mathcal{K}}$  is given by  $\sqrt{\gamma_0 \gamma_1}$ , with associated right eigenmatrix  $r$  and left one  $\ell$  being as follows:

$$r = \begin{pmatrix} \frac{\sqrt{\gamma_1}}{\sqrt{\gamma_1 + e^{-h} \sqrt{\gamma_0}}} & 0 \\ 0 & \frac{\sqrt{\gamma_0}}{\sqrt{\gamma_0 + e^h \sqrt{\gamma_1}}} \end{pmatrix},$$

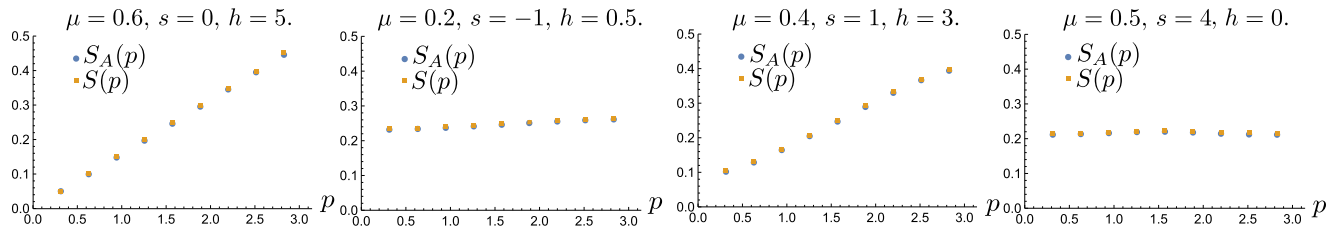


FIG. 6. Comparison between the exact structure factor  $S(p)$  and the approximated one  $S_A(p)$  for an XX chain with  $L = 10$  and different combinations of the various parameters. The good agreement between the two quantities shows that one can rely on this approximation to gain insight on the structure of the various ensembles.

$$\ell = \frac{1}{2} \begin{pmatrix} \frac{\sqrt{\gamma_1 + e^{-h}} \sqrt{\gamma_0}}{\sqrt{\gamma_1}} & 0 \\ 0 & \frac{\sqrt{\gamma_0 + e^h} \sqrt{\gamma_1}}{\sqrt{\gamma_0}} \end{pmatrix}.$$

Given any operator  $x$  acting on the first  $L - 1$  sites of the chain, one has  $\mathcal{K}[x \otimes r] = \sqrt{\gamma_0 \gamma_1} x \otimes r$ . This shows that the eigenvalue  $\sqrt{\gamma_0 \gamma_1}$  is highly degenerate. Taking into account this degeneracy when applying perturbation theory, one has that the eigenvalue with the largest real part of the tilted operator, which is the cumulant generating function  $\psi(s, h)$ , is given by

$$\psi(s, h) = \sqrt{\gamma_0 \gamma_1} e^{|s|} + w(h) + O(e^{-|s|}), \quad (\text{B2})$$

where  $w(h)$  is the (possibly  $h$ -dependent) eigenvalue with the largest real part of the matrix

$$w_{ij} = \text{Tr}(\mathbf{e}_i^\dagger \otimes \ell \mathcal{W}[\mathbf{e}_j \otimes r]),$$

with  $\mathbf{e}_i$  being an element of an operator basis for the first  $L - 1$  sites of the chain, such that  $\text{Tr}(\mathbf{e}_i^\dagger \mathbf{e}_j) = \delta_{i,j}$ . Because of the fact that  $\ell r = r \ell = \mathbf{1}_2/2$ , and because of the shape of the map  $\mathcal{W}$ , it is straightforward to show that the matrix  $[w_{ij}]$  actually does not depend on  $h$  and nor does its largest eigenvalue  $w(h)$ . The same holds true even if one considers the presence of an extra dephasing term in the Lindblad generator given by

$$\mathcal{L}^D[\rho] = \gamma_D \sum_{m=1}^L \left( n^{(m)} \rho n^{(m)} - \frac{1}{2} \{ \rho, n^{(m)} \} \right). \quad (\text{B3})$$

Since  $w(h)$  does not depend on  $h$ , for large biases towards active realizations ( $-s \gg 1$ ), the current, given by the first

derivative with respect to  $h$  of  $\psi(s, h)$  [cf. Eq. (B2)], is of order  $\langle q(t) \rangle_{s,h} = \partial_h \psi(s, h) \sim O(e^{-|s|})$ .

Given also that  $\langle k(t) \rangle_{s,h} = -\partial_s \psi(s, h) \approx e^{|s|}$ , one recovers, for large negative  $s$ , the diffusivelike scaling of the current with the average activity  $\langle q(t) \rangle_{s,h} \propto \frac{1}{\langle k(t) \rangle_{s,h}}$ .

### APPENDIX C: APPROXIMATION OF DENSITY-DENSITY CORRELATIONS FOR THE COMPUTATION OF THE STRUCTURE FACTOR

We show here by numerical evidence that, concerning the computation of the structure factor for the XX chain, we can approximate the expectation  $\langle O \rangle_{s,h} = \text{Tr}(O \ell_{s,h}^{1/2} r_{s,h} \ell_{s,h}^{1/2})$  with the functional  $\langle \langle O \rangle \rangle_{s,h} = \text{Tr}(\ell_{s,h} O r_{s,h})$ .

We verified this for systems with up to  $L = 10$  sites, always obtaining a satisfactory agreement between the structure factor  $S(p)$  computed via the exact correlations  $\langle n_m n_k \rangle_{s,h} - \langle n_m \rangle_{s,h} \langle n_k \rangle_{s,h}$  and the approximated structure factor  $S_A(p)$  computed with the correlations  $\langle \langle n_m n_k \rangle \rangle_{s,h} - \langle \langle n_m \rangle \rangle_{s,h} \langle \langle n_k \rangle \rangle_{s,h}$ . Indeed, as it is possible to appreciate from Fig. 6, there is a very nice agreement between the two. Moreover, from numerical results, we observed that the error made in computing density-density correlations between bulk sites with the approximated functional is smaller than the one made computing density correlations for sites next to the boundaries. Because of this, we expect the agreement between  $S(p)$  and  $S_A(p)$  to persist also for larger  $L$ , as bulk contributions become predominant.

- [1] H. Touchette, *Phys. Rep.* **478**, 1 (2009).
- [2] R. Chetrite and H. Touchette, *Ann. Henri Poincaré* **16**, 2005 (2015).
- [3] L. Bertini, A. De Sole, D. Gabrielli, G. Jona-Lasinio, and C. Landim, *Rev. Mod. Phys.* **87**, 593 (2015)
- [4] T. Bodineau and B. Derrida, *Phys. Rev. Lett.* **92**, 180601 (2004).
- [5] B. Derrida, *J. Stat. Mech.* (2007) P07023.
- [6] B. Derrida and A. Gerschenfeld, *J. Stat. Phys.* **137**, 978 (2009).
- [7] P. I. Hurtado, C. P. Espigares, J. J. del Pozo, and P. L. Garrido, *J. Stat. Phys.* **154**, 214 (2014).
- [8] D. Bernard and B. Doyon, *J. Stat. Mech.* (2016) 033104.
- [9] O. A. Castro-Alvaredo, B. Doyon, and T. Yoshimura, *Phys. Rev. X* **6**, 041065 (2016).
- [10] D. Karevski and G. M. Schütz, *Phys. Rev. Lett.* **118**, 030601 (2017).
- [11] Y. Baek, Y. Kafri, and V. Lecomte, *Phys. Rev. Lett.* **118**, 030604 (2017).
- [12] M. Ljubotina, M. Žnidarič, and T. Prosen, *Nat. Commun.* **8**, 16117 (2017).
- [13] C. Appert-Rolland, B. Derrida, V. Lecomte, and F. van Wijland, *Phys. Rev. E* **78**, 021122 (2008).
- [14] J. P. Garrahan, R. L. Jack, V. Lecomte, E. Pitard, K. van Duijvendijk, and F. van Wijland, *J. Phys. A: Math. Theor.* **42**, 075007 (2009).
- [15] J. P. Garrahan and I. Lesanovsky, *Phys. Rev. Lett.* **104**, 160601 (2010).
- [16] C. P. Espigares, P. L. Garrido, and P. I. Hurtado, *Phys. Rev. E* **87**, 032115 (2013).
- [17] R. L. Jack, I. R. Thompson, and P. Sollich, *Phys. Rev. Lett.* **114**, 060601 (2015).
- [18] M. Žnidarič, *J. Phys. A: Math. Theor.* **43**, 415004 (2010).

- [19] M. Žnidarič, *J. Stat. Mech.* (2010) L05002.
- [20] T. Prosen, *Phys. Rev. Lett.* **106**, 217206 (2011).
- [21] E. Iliovski and T. Prosen, *Nucl. Phys. B* **882**, 485 (2014).
- [22] T. Prosen and I. Pižorn, *Phys. Rev. Lett.* **101**, 105701 (2008).
- [23] L. Piroli, E. Vernier, and P. Calabrese, *Phys. Rev. B* **94**, 054313 (2016).
- [24] D. Karevski, V. Popkov, and G. M. Schütz, Matrix product ansatz for non-equilibrium quantum steady states, in *From Particle Systems to Partial Differential Equations: PSPDE IV, Braga, Portugal, December 2015*, edited by P. Gonçalves and A. J. Soares (Springer, Cham, 2017), pp. 221–245.
- [25] T. Prosen, *Phys. Rev. Lett.* **107**, 137201 (2011).
- [26] M. Žnidarič, *Phys. Rev. Lett.* **112**, 040602 (2014).
- [27] M. Žnidarič, *Phys. Rev. E* **89**, 042140 (2014).
- [28] M. Žnidarič, *Phys. Rev. B* **90**, 115156 (2014).
- [29] D. Manzano and P. Hurtado, [arXiv:1707.07895](https://arxiv.org/abs/1707.07895).
- [30] F. Carollo, J. P. Garrahan, I. Lesanovsky, and C. Pérez-Espigares, *Phys. Rev. E* **96**, 052118 (2017).
- [31] V. Lecomte, C. Appert-Rolland, and F. van Wijland, *Phys. Rev. Lett.* **95**, 010601 (2005).
- [32] V. Lecomte, C. Appert-Rolland, and F. van Wijland, *J. Stat. Phys.* **127**, 51 (2007).
- [33] J. P. Garrahan, *J. Stat. Mech.* (2016) 073208.
- [34] G. Lindblad, *Commun. Math. Phys.* **48**, 119 (1976).
- [35] V. Gorini, A. Kossakowski, and E. C. G. Sudarshan, *J. Math. Phys.* **17**, 821 (1976).
- [36] F. Carollo, J. P. Garrahan, I. Lesanovsky, and C. Pérez-Espigares, *Phys. Rev. A* **98**, 010103(R) (2018).
- [37] V. Eisler, *J. Stat. Mech.* (2011) P06007.
- [38] K. Temme, M. M. Wolf, and F. Verstraete, *New J. Phys.* **14**, 075004 (2012).
- [39] T. Prosen, *New J. Phys.* **10**, 043026 (2008).
- [40] T. Prosen, *J. Stat. Mech.* (2010) P07020.
- [41] R. Chetrite and H. Touchette, *Phys. Rev. Lett.* **111**, 120601 (2013).
- [42] J. de Gier and F. H. L. Essler, *Phys. Rev. Lett.* **95**, 240601 (2005).
- [43] J. de Gier and F. H. L. Essler, *Phys. Rev. Lett.* **107**, 010602 (2011).
- [44] M. Gorissen, A. Lazarescu, K. Mallick, and C. Vanderzande, *Phys. Rev. Lett.* **109**, 170601 (2012).
- [45] D. Manzano, M. Tiersch, A. Asadian, and H. J. Briegel, *Phys. Rev. E* **86**, 061118 (2012).
- [46] V. Popkov, S. Essink, C. Presilla, and G. Schütz, [arXiv:1806.10422](https://arxiv.org/abs/1806.10422).
- [47] D. Bernard, T. Jin, and O. Shpielberg, *Europhys. Lett.* **121**, 60006 (2018).
- [48] V. Popkov and G. M. Schütz, *J. Stat. Phys.* **142**, 627 (2011).
- [49] S. Torquato, *Phys. Rev. E* **94**, 022122 (2016).
- [50] T. Prosen and M. Žnidarič, *Phys. Rev. Lett.* **105**, 060603 (2010).